

Stem Cell Reports, Volume 10

Supplemental Information

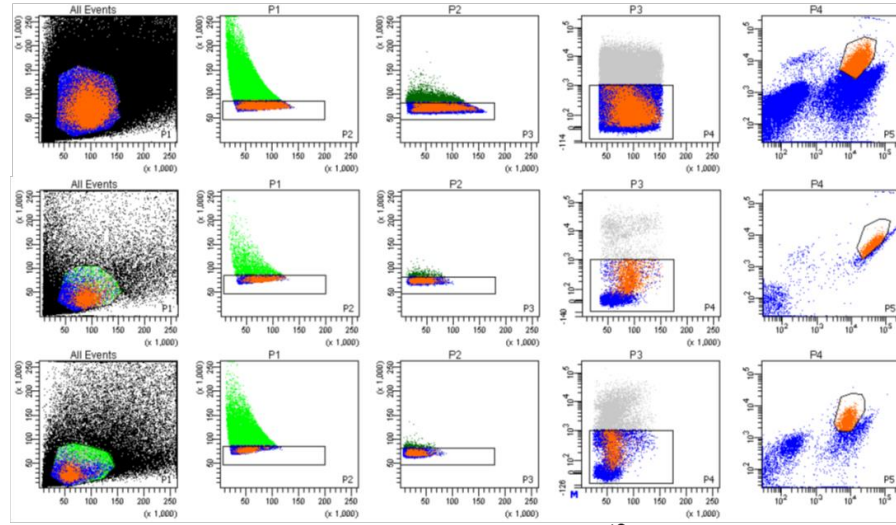
High-Yield Purification, Preservation, and Serial Transplantation of Human Satellite Cells

Steven M. Garcia, Stanley Tamaki, Solomon Lee, Alvin Wong, Anthony Jose, Joanna Dreux, Gayle Kouklis, Hani Sbitany, Rahul Seth, P. Daniel Knott, Chase Heaton, William R. Ryan, Esther A. Kim, Scott L. Hansen, William Y. Hoffman, and Jason H. Pomerantz

High-yield purification, preservation and serial transplantation of human satellite cells: Supplementary Information

A

With CD29/CD56 only



SSC
FSC

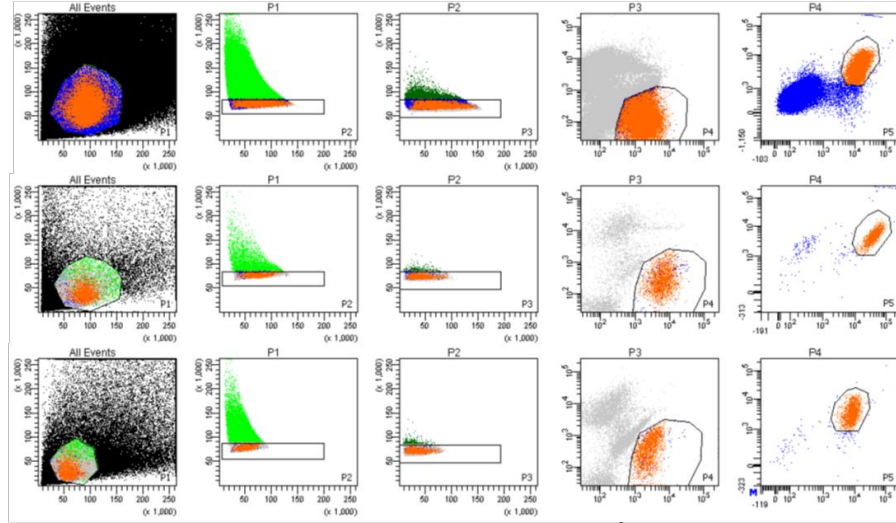
FSC-W
FSC-H

SSC-W
SSC-H

Sytox CD31/34/45
FSC

CD56
CD29

With CD29/CD56 plus CXCR4



SSC
FSC

FSC-W
FSC-H

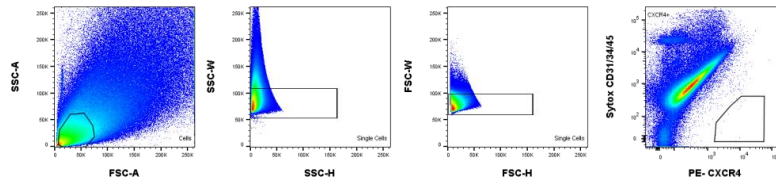
SSC-W
SSC-H

Sytox CD31/34/45
CXCR4

CD56
CD29

B

FMO



CXCR4

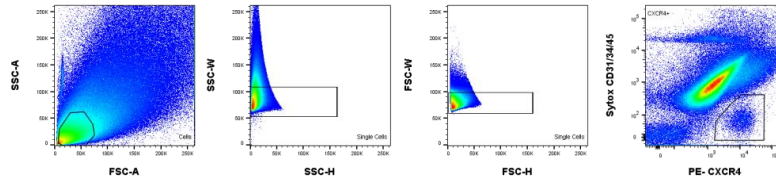


Figure S1 Related to Figure 1. (a) Six example representative flow cytometry profiles of HuSC isolation utilizing positive selection with CD29 and CD56 only compared with CXCR4 plus CD29 and CD56, illustrating flow profiles with of satellite cell location with various sample preparations. The first three rows illustrate representative flow profiles of isolations without utilizing CXCR4. The first row profile demonstrates a sample preparation resulting in unclear left, right, and lower margins for the CD56+CD29+ HuSC population. The second and third row profiles demonstrate sorts with improved clarity of the HuSC population; however, the lower margin still remains unclear. Rows four through six are representative flow profiles utilizing the combination of CXCR4, CD29, and CD56. These three examples demonstrate improved separation of the HuSC population from non-satellite cells, resulting in less arbitrary gating as seen in the example profiles in which CXCR4 was not used. The use of all three positive selection markers is indeed still necessary for less common cases where sample preparations result in profiles like row four, where the HuSC population separation is less evident. **(b)** Fluorescence minus one (FMO) sorting of human muscle without (top) and with (bottom) CXCR4 antibody. Gated area in the far-right bottom panel shows CXCR4 positive cells.

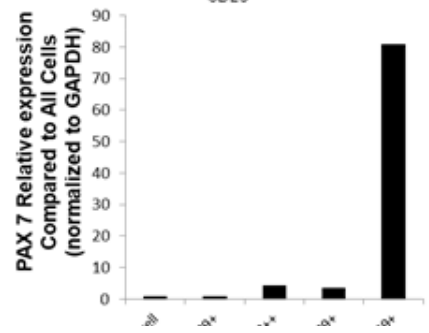
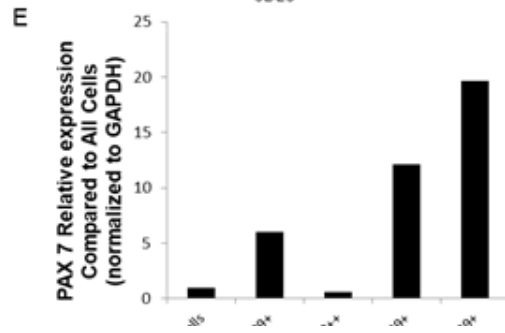
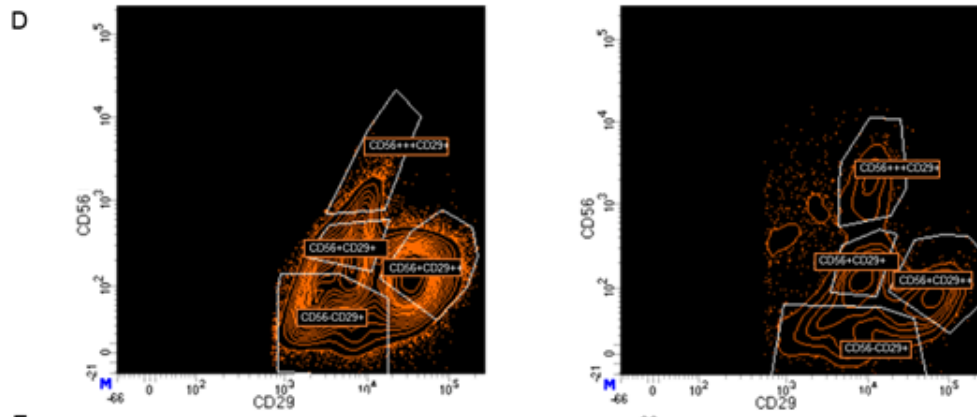
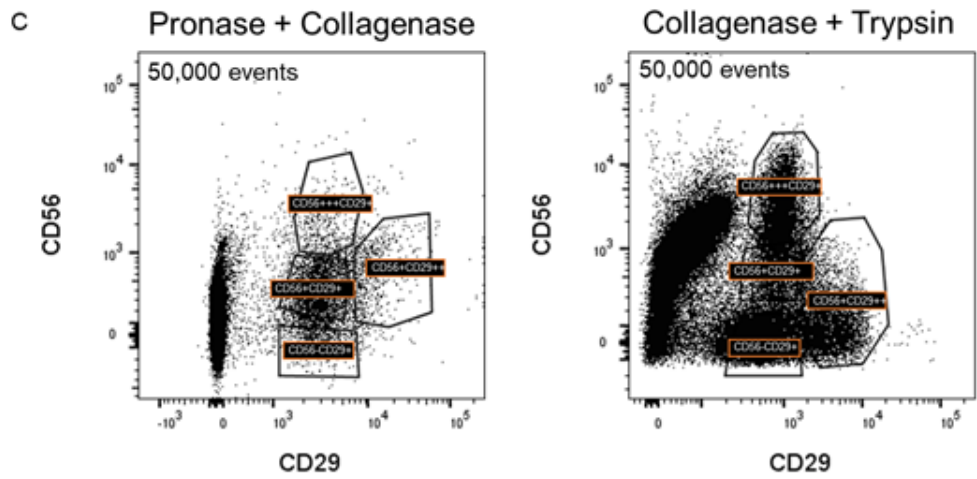
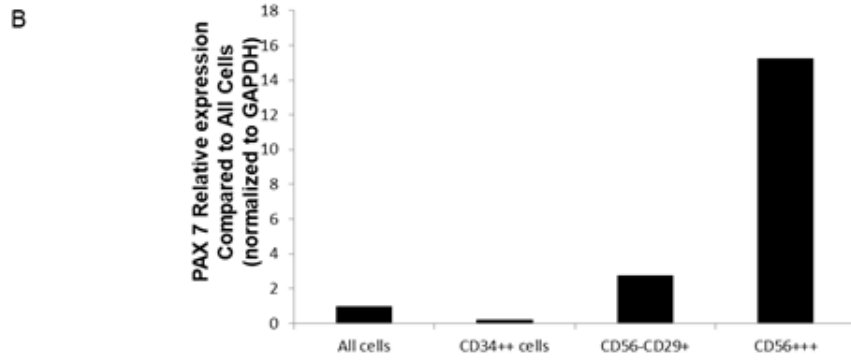
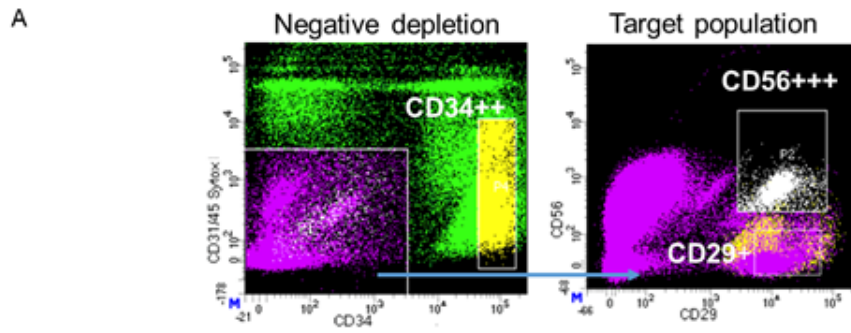


Figure S2 Related to Figure 1. Improvements in the isolation of human satellite cells. **(a)** Human satellite cells are CD34-negative by flow cytometry and CD34-positive cells are PAX7-negative. Singlets were sorted for sytox-/CD31-/CD45-/CD34-negative cells and CD34⁺⁺ cells. Sytox-/CD31-/CD45-/CD34- cells were then separated based on expression of CD29 and CD56. **(b)** PAX7 expression assessed by qRT-PCR of populations within the digestions shown in (a) as compared to all cells. CD 56⁺⁺⁺/CD29⁺ cells were enriched for satellite cells as determined by the largest PAX7 expression. CD34⁺⁺ cells are PAX7-negative. The qRT-PCR was performed in technical triplicates. **(c)** Collagenase followed by trypsin enzymatic digestion of human muscle compared with digestion by pronase and collagenase. Representative profiles of human muscle digested with pronase and collagenase compared with collagenase and trypsin shown with identical numbers of events. In the pronase / collagenase plot the majority of events reside in the far-left cluster. **(d)** Another representative flow cytometry profile of digestions utilizing pronase / collagenase and collagenase / trypsin shown using zebra plots. Cells were gated for live singlets, depleted of CD31/34/45, and CD29⁺ cells were gated for display in the profiles shown. Profiles were split into 4 areas and cells were sorted from each for qRT-PCR and compared to mRNA from unsorted cells (all cells); CD56-CD29⁺, CD56⁺CD29⁺⁺, CD56⁺CD29⁺, and CD56⁺⁺⁺CD29⁺. **(e)** PAX7 expression assessed by qRT-PCR of populations within the digestions shown in (a) as compared to unsorted cells. The qRT-PCR was performed in technical triplicates. Positive selection with CXCR4 was not used in development of this aspect of the isolation protocol.

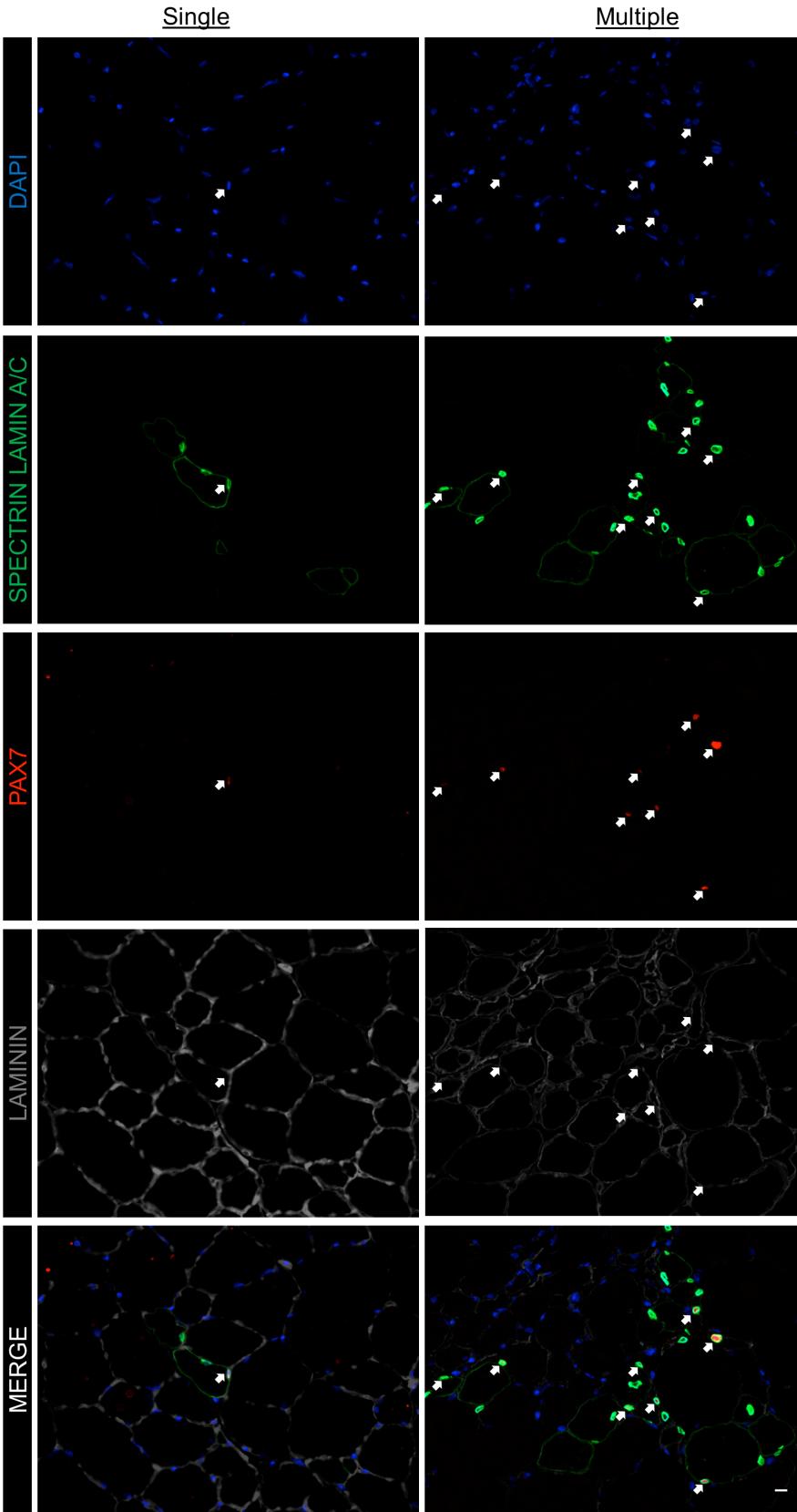


Figure S3 Related to Figure

2. All immunofluorescence panels for the merged image shown in Fig. 2c. Single and multiple injection transplant mice were stained for human engraftment and PAX7 cells with DAPI (blue), SPECTRIN and LAMIN A/C (green), PAX7 (red), and Laminin (grey). Human PAX7-positive satellite cells are marked with arrows. Scale bar 10 μ m.

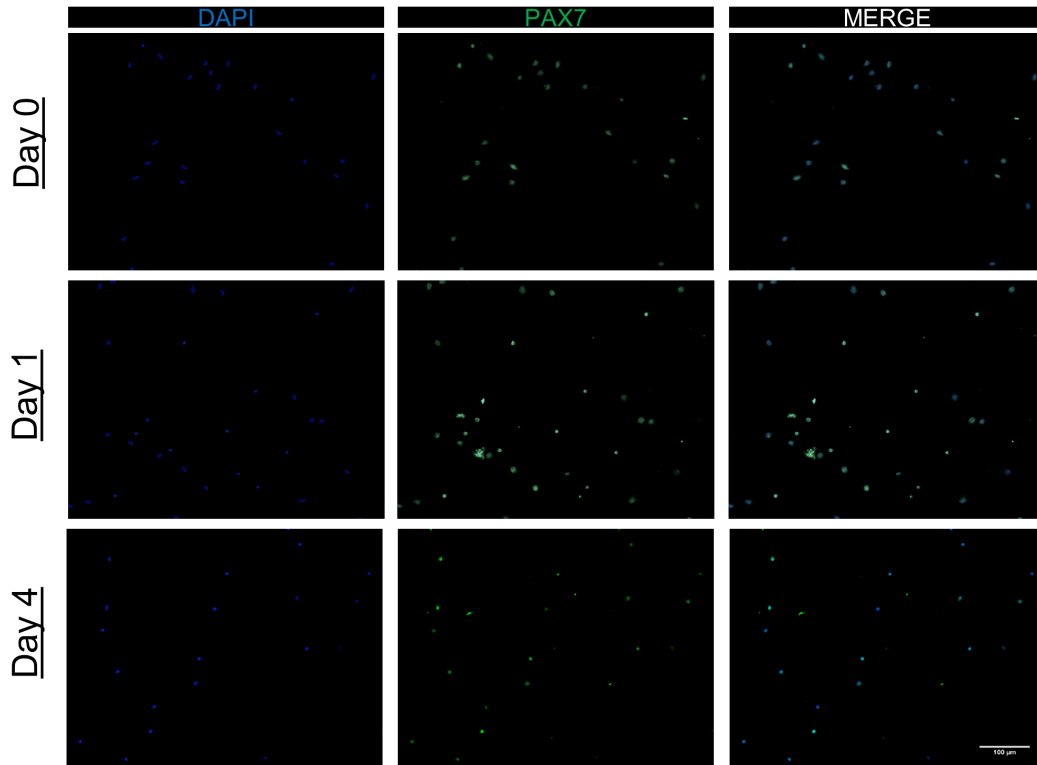


Figure S4 Related to Figure 3. Representative images of PAX7 expression staining from cells isolated on day 0, day 1, and day 4 in Fig 3d. DAPI, PAX7, and merged channels are shown separately. Scale bar 100 μ m.

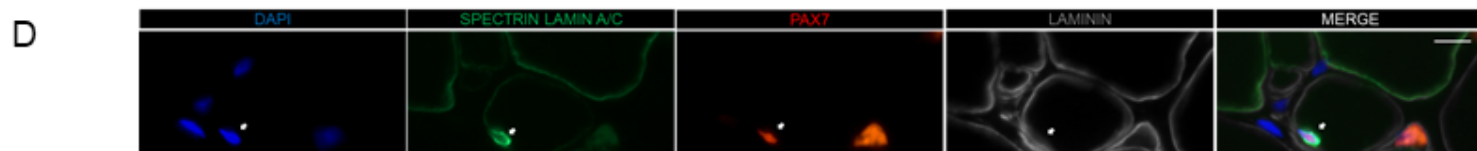
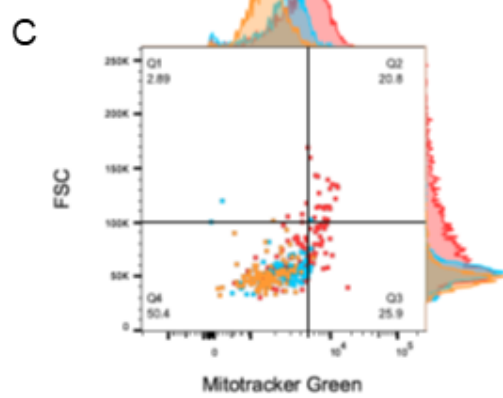
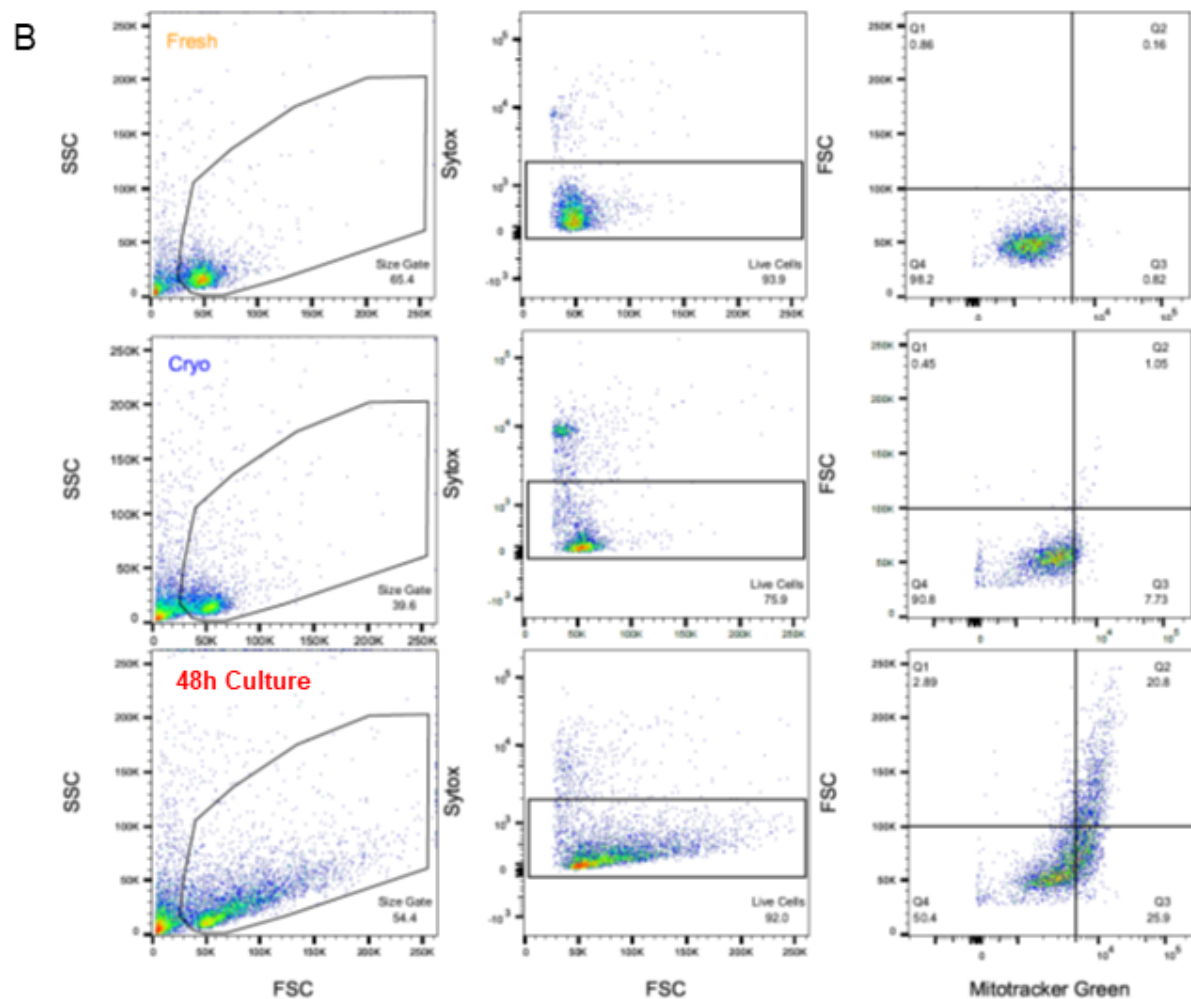
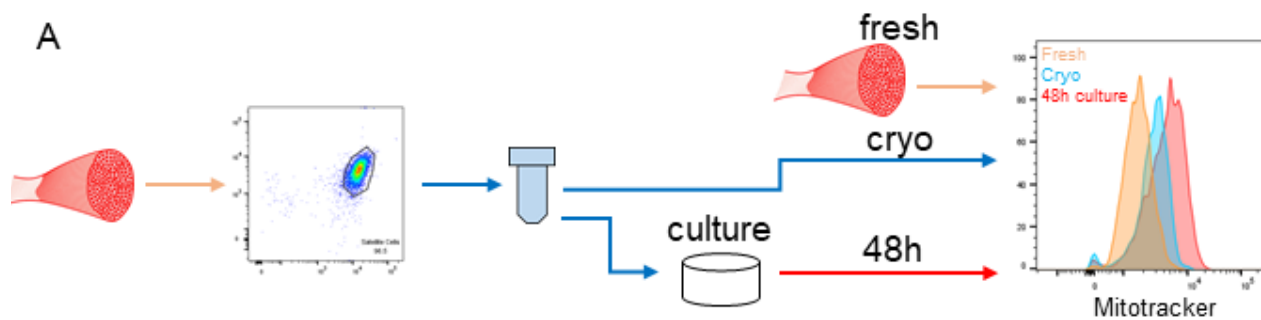


Figure S5 Related to Figure 5. Mitochondrial activity of cryopreserved human satellite cells compared to freshly isolated and 48h cultured cells. **(a)** Schematic of experimental procedure for MitoTracker Green experiments. Cryopreserved cells were directly compared to 48h cultured cells. All cells were originally cryopreserved and split into either the culture group or thawed and tested immediately. Experiments were timed to allow flow cytometry analysis on the same experimental day. Cryopreserved and 48h cultured cells were compared to freshly isolated cells of another rectus abdominis muscle on the same day for an additional control. **(b)** Representative flow cytometry profiles for all three experimental conditions as described. **(c)** Merged profiles demonstrating differences among fresh (orange), cryo (blue), and 48h cultured satellite cells (red). Merged flow cytometry plots from all 3 groups in (b) comparing relative size with forward scatter (FSC) and relative mitochondrial activity (MitoTracker Green). Adjunct histograms for FSC and Mitrotracker green are shown on the right and top of the plot respectively. **(d)** All immunofluorescence panels for the merged image shown in Fig. 5h. Transplanted mice were stained for human engraftment and PAX7 cells with DAPI (blue), SPECTRIN and LAMIN A/C (green), PAX7 (red), and Laminin (grey). Human PAX7-positive satellite cells are marked with arrows. Scale bar 10 μm .

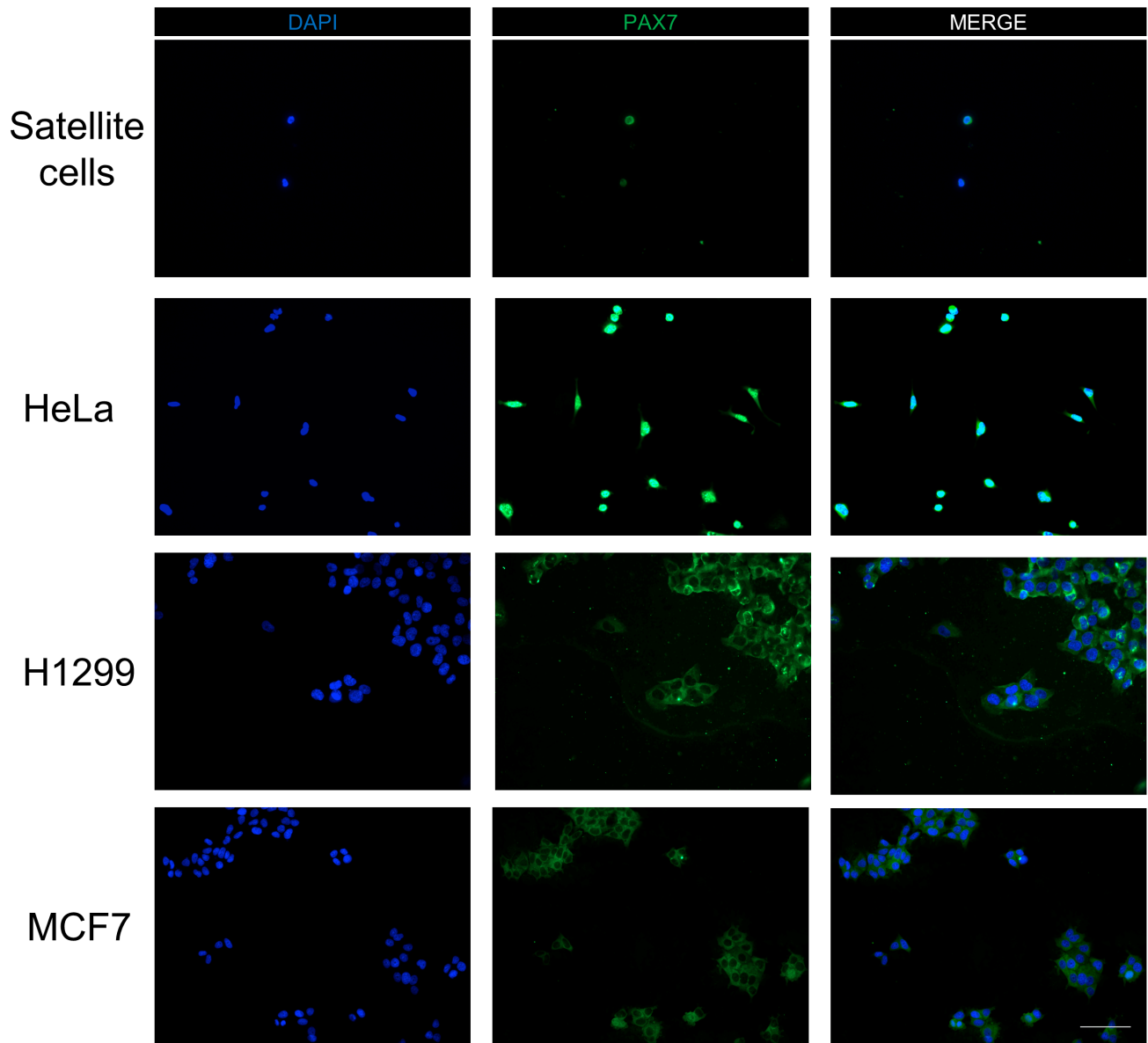


Figure S6 Related to Figure 1. Representative images of PAX7 staining utilizing the anti-PAX7 Abcam (ab92317) antibody on human satellite cells, HeLa cells, H1299 cells, and MCF7 cells. DAPI, PAX7, and merged channels are shown separately. (Note, HeLa cells can express PAX7 as shown here, and separately by RT-PCR). Scale bar 100 μm .

| Sex | Age | muscle | Satellite cell # | gm | Per gm |
|-----|-----|--------------------------------|------------------|------|--------|
| M | 43 | Bicep | 43186 | 2 | 21593 |
| M | 67 | Bicep | 17929 | 2 | 8965 |
| F | 57 | Brachioradialis | 1936 | 0.6 | 3227 |
| M | 72 | Brachioradialis | 38006 | 3.7 | 10272 |
| M | 72 | Flexor carpi radialis | 1901 | 2.21 | 860 |
| M | 76 | Flexor digitorum superficialis | 1755 | 1.05 | 1671 |
| M | 59 | Flexor hallucis longus | 5671 | 0.57 | 9949 |
| M | 20 | Gastrocnemius | 7508 | 0.58 | 12945 |
| M | 43 | Gastrocnemius | 20906 | 2 | 10453 |
| M | 59 | Gastrocnemius | 9525 | 1 | 9525 |
| M | 67 | Gastrocnemius | 9694 | 2 | 4847 |
| F | 86 | Gluteus maximus | 4429 | 0.4 | 11073 |
| M | 47 | Gluteus maximus | 12080 | 0.71 | 17014 |
| M | 66 | Grac/SemiT | 14336 | 0.63 | 22756 |
| F | 43 | Latissimus | 20866 | 2 | 10433 |
| F | 73 | Latissimus | 10744 | 2 | 5372 |
| M | 43 | Pectoralis major | 47405 | 2 | 23703 |
| M | 67 | Pectoralis major | 8278 | 2 | 4139 |
| M | 67 | Pectoralis major | 2986 | 5 | 597 |
| M | 50 | Peroneus | 36850 | 6 | 6142 |
| M | 20 | Psoas | 9282 | 0.67 | 13854 |
| F | 37 | Rectus abdominis | 7923 | 1.96 | 4042 |
| F | 42 | Rectus abdominis | 29990 | 0.7 | 42843 |
| F | 44 | Rectus abdominis | 22908 | 1.41 | 16247 |
| F | 45 | Rectus abdominis | 3929 | 2 | 1965 |
| F | 46 | Rectus abdominis | 22285 | 3.15 | 7075 |
| F | 58 | Rectus abdominis | 122215 | 5.65 | 21631 |
| M | 26 | Rectus abdominis | 1932 | 1.29 | 1498 |
| M | 43 | Rectus abdominis | 21633 | 2 | 10817 |
| M | 46 | Rectus abdominis | 2008 | 0.52 | 3862 |
| M | 51 | Rectus abdominis | 16881 | 1.66 | 10169 |
| M | 51 | Rectus abdominis | 31987 | 1.77 | 18072 |
| M | 51 | Rectus abdominis | 16041 | 3.06 | 5242 |
| M | 51 | Rectus abdominis | 18928 | 3.11 | 6086 |
| M | 56 | Rectus abdominis | 14191 | 1.9 | 7469 |
| M | 67 | Rectus abdominis | 6130 | 2 | 3065 |
| M | 85 | Rectus abdominis | 15520 | 2.9 | 5352 |
| M | 66 | Sartorius | 21741 | 0.51 | 42629 |
| F | 86 | Serratus anterior | 6038 | 1.4 | 4313 |
| F | 71 | Soleus | 148796 | 3.6 | 41332 |
| M | 43 | Temporalis | 18867 | 2 | 9434 |
| M | 67 | Temporalis | 10698 | 2 | 5349 |
| M | 59 | Tongue | 4409 | 0.3 | 14697 |
| M | 67 | Tongue | 3012 | 0.21 | 14343 |
| M | 35 | Trapezius | 2189 | 3.5 | 625 |
| F | 51 | Vastus lateralis | 1287 | 0.88 | 1463 |
| F | 61 | Vastus lateralis | 23014 | 0.98 | 23484 |
| M | 43 | Vastus lateralis | 23052 | 2 | 11526 |
| M | 50 | Vastus lateralis | 20417 | 1.8 | 11343 |
| M | 56 | Vastus lateralis | 72777 | 3.55 | 20501 |
| M | 59 | Vastus lateralis | 15943 | 1.44 | 11072 |
| M | 59 | Vastus lateralis | 28484 | 1.82 | 15651 |
| M | 67 | Vastus lateralis | 6697 | 2 | 3349 |
| M | 70 | Vastus lateralis | 10275 | 1.52 | 6760 |
| M | 70 | Vastus lateralis | 21323 | 1.88 | 11342 |
| M | 73 | Vastus lateralis | 4311 | 2 | 2156 |
| M | 81 | Vastus lateralis | 7679 | 3.6 | 2133 |

Table S1 Related to Figure 1. Fifty-seven adult muscle samples were processed from 20 different muscle types. The samples were obtained from both genders, 43 male and 14 female. Age at time of donation ranged from 20 to 86 years. Gm – weight in grams of the sample. Per gm – number of HuSCs isolated per gm of sample.

| Variable | Statistical Test | P-Value |
|--------------------------------|--------------------------------|----------------|
| Gender | Two-tailed T Test | 0.209 |
| Age | Linear Regression | 0.474 |
| Age (grouped) | One-way ANOVA | 0.610 |
| Muscle Type | One-way ANOVA | 0.052 |
| Muscle Weight | Linear Regression | 0.304 |
| Muscle Weight (grouped) | One-way ANOVA | 0.180 |
| | | |
| | Multivariate Regression | P-Value |
| Gender | | 0.218 |
| Age | | 0.521 |
| Muscle Type | | 0.847 |
| Muscle Weight | | 0.348 |

Table S2 Related to Figure 1. Statistical analysis for differences in satellite cells isolated per gram of muscle as a function of gender, age, muscle type, and muscle weight.

| Antibody | Reactivity | Fluorophore | Company | Catalog Number |
|-----------------|-------------------|--------------------|-----------------|-----------------------|
| CD31 | Human | Metal beads | Miltenyi Biotec | 130-091-935 |
| CD45 | Human | Metal beads | Miltenyi Biotec | 130-045-801 |
| CD31 | Human | 450 | Ebioscience | 48-0319-42 |
| CD34 | Human | 450 | Ebioscience | 48-0349-42 |
| CD45 | Human | 450 | Ebioscience | 48-0459-42 |
| CD56 | Human | APC-vio770 | Miltenyi Biotec | 130-100-694 |
| CD29 | Human | APC | Ebioscience | 17-0299-42 |
| CD29 | Human | FITC | Ebioscience | 11-0299-42 |
| CXCR4 | Human | APC | Ebioscience | 17-9999-42 |
| CXCR4 | Human | PE | Ebioscience | 12-9991-82 |
| CD31 | Mouse | 450 | Ebioscience | 12-0311-82 |
| CD45 | Mouse | 450 | Ebioscience | 12-0451-82 |
| Sca1 | Mouse | 450 | Ebioscience | 12-5981-81 |

Table S3 Related to Experimental Procedures. Antibodies used for human satellite cell isolations.

| Antibody | Reactivity | Company | Catalog Number |
|-------------------|-------------|---------------------|----------------|
| DYSTROPHIN | Human | DSHB | MANDYS104(7F7) |
| Dystrophin | Human/Mouse | DSHB | MANDRA1(7A10) |
| PAX7 | Human/Mouse | DSHB | PAX7 |
| PAX7 | Human/Mouse | Abcam | ab92317 |
| Laminin | Human/Mouse | Sigma-Aldrich | L9393 |
| SPECTRIN | Human | Leica Microsystems | NCL-SPEC1 |
| LAMIN A/C | Human | Vector Laboratories | VP-L550 |

Table S4 Related to Experimental Procedures. Antibodies used for immunofluorescence imaging.

| Target | Forward | Reverse |
|--------------|--|------------------------|
| GAPDH | GGCGCTGAGTACGTCGTG | GTCTTCTGGGTGGCAGTGATG |
| RPS13 | GTTGCTGTTTCGAAAGCATCTTG | AATATCGAGCCAAACGGTGAA |
| PAX7 | CCCCCGCACGGGATT | TATCTTGTGGCGGATGTGGTTA |
| MYF5 | CCACCTCCAACCTGCTCTGAT | TGATCCGGTCCACTATGTTG |
| MYOD1 | CCGCCTGAGCAAAGTAAATGA | GCAACCGCTGGTTTGGATT |
| MYOG | GCGGGCGGCCACACTGA | GGGGGCTCGCAAGGATG |
| CDC45 | IDT PrimeTime Predesigned qPCR Assay: Hs.PT.58.21113859 | |

Table S5 Related to Experimental Procedures. qRT-PCR primers used in this study.

Supplemental Experimental Procedures

Animal Care and Transplantation Studies. All mice were bred and housed in a pathogen-free facility at UCSF. All procedures were approved and performed in accordance with the UCSF Institutional Animal Care and Use Committee. All experiments were unblinded and performed in 8-12 week-old NOD.Cg-Prkdcscid Il2rgtm1Wjl/SzJ (NSG) mice (The Jackson Laboratory) and NSG mice crossed with C57BL/10ScSn-Dmdmdx/J (MDX) mice (The Jackson Laboratory), creating (NSG/MDX) mice. Mice were randomized to all experimental groups by sex and littermates and were pretreated with 18 gamma (Gy) on the day before transplantation. A 5 mm incision was made in the mouse skin overlying the TA muscle and HuSCs were injected along with 50 μ l 0.5% bupivacaine directly into the muscle of one leg. For cell injection, a 31 gauge needle on a 50 μ l Hamilton syringe was used. Equal numbers of cells were injected into each experimental leg within experiments, but varied slightly between experiments as indicated in the text. The skin was closed with sutures and skin glue was applied over the incision. When multiple injections were utilized, HuSCs were suspended in 50 μ l of in 0.5% bupivacaine and then subsequently transplanted in nine injections of approximately 5.5 μ l per NSG TA. The transplant sites were spaced evenly apart in a grid of three by three injections, covering the majority of the TA muscle. Transplanted TA muscles were

harvested at designated time points after transplantation. Harvested muscles were frozen in isopentane chilled in liquid nitrogen.

Serial 6 μ m transverse sections of the whole muscle were analyzed.

CXCR4+/CD29+/CD56+ Satellite Cell Sorting. Freshly harvested human muscle was either immediately digested or stored in DMEM with 30% FBS at 4°C. Muscle was trimmed of excess fat, tendon, connective tissue, and fascia and mechanically minced. The tissue was then digested in 1 mg/ml collagenase XI (Sigma-Aldrich) in Dulbecco's Modified Eagle Medium (DMEM) with high glucose, 10% FBS and 1% Penicillin / Streptomycin at 37°C for 70 minutes with intermittent manual needle trituration, performed slowly with an 18-gauge needle. Digests were washed with PBS and further digested with 0.25% trypsin at 37°C for 12-15 minutes. Suspensions were passed through 40 μ m nylon mesh, erythrocytes were lysed with ACK lysing buffer (ThermoFisher) for 5-7 minutes on ice, and washed with PBS. Magnetic column depletion of hematopoietic and endothelial cells was performed after cells were stained with anti-CD45 and anti-CD31 magnetic beads (Miltenyi Biotec). This step has the added benefit of removing small fiber fragments and fascial tissue, which are a cause of high background on the flow cytometer. Unbound cells were washed and stained with anti-CD29-488 or 647 (Ebioscience), anti-CD31-450 (Ebioscience), anti-CD34-450 or PE (Ebioscience), anti-CD45-450 (Ebioscience), anti-CD56-APC-vio-770 (Miltenyi Biotec), and anti-CXCR4-PE or APC (Ebioscience) (*Note* for the reisolation of HuSCs from transplanted mice: mouse muscle was processed as stated for human muscle, stained with the following antibodies: anti-human CD29-488 or 647 (Ebioscience), anti-human CD31-450 (Ebioscience), anti-human CD45-450 (Ebioscience), anti-human CD56-APC-vio-770 (Miltenyi Biotec), anti-human CXCR4-PE or APC (Ebioscience), anti-mouse CD31-450 (Ebioscience), anti-mouse CD45-450 (Ebioscience), and anti-mouse Sc α 1-450 (Ebioscience)). Cells were washed and resuspend in flow cytometry buffer with 1:1000 sytox blue (Invitrogen). Flow cytometry antibodies listed in Supplementary Table 3. Flow cytometry analysis and cell sorting were performed at the University of California San Francisco Flow Cytometry Core with the BD FACSAria2 operated using FACSDiva software. Viable cells were gated using sytox and singlet cells were based on scattering to avoid cell clusters. First, cells incubated with isotype antibodies were analyzed to determine gating. Then, viable cells were depleted for CD31, CD34, and CD45 expressing cells. Cells that remained after depletion were sorted for CXCR4+/CD29+/CD56+ and collected for further experimentation. We have previously published FMO controls for CD56 and CD29 use in HuSC isolation (Xu et al., 2015). Cells were sorted in 20% FBS in DMEM supplemented with 10 μ M Rho-associated protein kinase inhibitor (ROCKi) (Y-27632 2HCl, Selleck Chemicals). See (Garcia et al., 2017; Xu et al., 2015) for details of the authors' prior muscle digestion and HuSC isolation protocol. Flow cytometry isolations were analyzed with FACSDiva and FlowJo software.

PAX7 immunostaining of cells from digested muscle. Sorted cells were collected in 20% FBS-DMEM with 10 mM ROCKi and plated directly into wells of BioCoated laminin-coated chamber slides (BD Biosciences) previously coated for 1 hr with extracellular matrix gel (1:100, Sigma-Aldrich) in DMEM at a density of 5,000 cells per 0.7 cm² well. The cells were incubated in the chamber slides for 3 hours at 37°C with 5% CO₂ to allow for attachment. The cells were washed with PBS and then fixed in 4% PFA for 20 min. Cells were washed with 0.1% Tween-20 in PBS and blocked with protein-free serum block (DAKO). Slides were stained with monoclonal rabbit anti-PAX7 antibody (1:500, Abcam) overnight at room temperature (See **Supplementary Fig. 6** for antibody controls). Immunostaining antibodies listed in Supplementary Table 4. Slides were washed with 0.1% Tween-20 in PBS and then incubated with FITC donkey anti-rabbit (1:300 Jackson Immunology) for 1 hour at room temperature. Slides were washed again and mounted with VECTASHIELD mounting medium with DAPI (Vector Laboratories).

NSG TA analysis.

All glass slides were removed from -80°C and warmed at room temperature for 10 min. For hematoxylin and eosin (H&E) staining, slides were rinsed with water and dried. Sections were then dehydrated as follows; 5 min in xylenes, twice; 5 min in 100% ethanol, twice; 5 min in 95% ethanol; 5 min in 80% ethanol and washed in water for 30 s. Slides were then placed in 3x Gill's Hematoxylin for 4 min and washed with water for 30 s. For nuclear staining, slides were placed in Scott's water for 3 min and washed in water for 30 s. Slides were then placed in Eosin for 2 min and washed with water for 30 s. Sections were dehydrated again as follows: 1 min 80% ethanol; 2 min 95% ethanol, twice; 3 min 100% ethanol, twice; 2 min xylenes, twice. Slides were then mounted with Permount and cover slips and air-dried overnight before imaging. All samples were examined using a Leica upright microscope and muscle area was analyzed using ImageJ (ImageJ, U. S. National Institutes of Health). For human DYSTROPHIN immunostaining, sections were fixed in 4% PFA for 10 min at room temperature and then washed in PBST (PBS with 0.1% Tween-20 (Sigma-Aldrich)). The sections were blocked with 10% goat serum in PBS for 10 min at room temperature. The sections were then incubated overnight at room temperature with mouse monoclonal anti-human DYSTROPHIN (1:10 DSHB), human specificity of which was previously confirmed (Xu et al., 2015). The sections were then washed in PBST followed by 1 hr of incubation at room temperature with Alexa Fluor 594 goat anti-mouse IgG (1:500 Thermo) in 10% normal goat serum in PBS. Sections were mounted with VECTASHIELD mounting medium with DAPI (Vector Laboratories) and all samples were examined using a Leica upright microscope. Human-derived fibers (e.g. hDYSTROPHIN positive) were quantified by counting the number of positively stained fibers in the section with the most positive fibers after analyzing sections along the length of the muscle as has been previously reported (Rozkalne et al., 2014; Xu et al., 2015). For all other immunostainings, the slides were fixed in 4% PFA at room temperature for 10 min, washed in PBST, and then blocked

with protein-free serum block (DAKO) and incubated at room temperature overnight with the following primary antibodies: mouse monoclonal IgG1 anti-PAX7 (1:10 DSHB), rabbit polyclonal anti-Laminin (1:250 Sigma-Aldrich), rabbit polyclonal anti-pan Dystrophin (1:500 Thermo), mouse monoclonal IgG2b anti-human SPECTRIN (Leica Microsystems), mouse monoclonal IgG2b anti-human LAMIN A/C (Vector Laboratories). Immunostaining antibodies listed in Supplementary Table 4. After PBST wash the following corresponding secondary antibodies were applied for 1 hr at room temperature: FITC donkey anti-mouse (1:500 Jackson Immunology), Cy3 goat anti-mouse (1:500 Jackson Immunology), Cy5 donkey anti-mouse (1:500 Jackson Immunology), Cy5 donkey anti-rabbit (1:300 Jackson Immunology), Alexa Fluor 488 goat anti-mouse IgG1 (1:500 Thermo), Alexa Fluor 594 goat anti-mouse IgG1 (1:500 Thermo), Alexa Fluor 488 goat anti-mouse IgG2b (1:500 Thermo), Alexa Fluor 594 goat anti-mouse IgG2b (1:500 Thermo). Sections were mounted with VECTASHIELD mounting medium with DAPI (Vector Laboratories) and all samples were examined using a Leica upright microscope.

NSG/MDX Mouse Line Derivation. C57BL/10ScSn-Dmdmdx/J (MDX) (Jackson Laboratories) homozygous females were mated with male NOD.Cg-Prkdcscid Il2rgtm1 Wjl/SzJ (NSG) mice (Jackson Laboratories). Male offspring from this cross were screened for recombination between the MDX and IL2R gamma mutation by PCR amplification of mutant and wildtype alleles. Approximately 1 in 20 males were recombinants and these were backcrossed to NSG females for a total of 6 generations. Each generation was genotyped by PCR. Starting with the 4th generation, screening for SCID mutants was performed by phenotype assay via flow cytometry to confirm the absence of T cells and B cells in mouse blood samples with CD3 and CD20 respectively in the recombinant mice. In adult mice the MDX is phenotype became apparent at 10 weeks of age by enlarged shoulder muscles. NSG/MDX females are fertile and the brown coat color can be maintained in MDX/NSG mice, which increases their survival after weaning. Screening for the MDX mutation (Shin et al., 2011) was performed with the following primers: (1) Wild-Type Reverse: GATACGCTTTAATGCCTTTAGTCACTCAGATAGTTGAAGCCAT, (2) Mutant-Reverse: CGGCCTGTCACTCAGATAGTTGAAGCCATTTTA, (3) Common Forward: GCGCGAAACTCATCAAATATGCGTGTTAGTGT; with the following PCR protocol: 95°C for 7 min, 30 x (95°C for 20 sec, 59°C for 30 sec, 72°C for 40 sec), 72°C for 3 min, 4°C hold. Product Sizes: MDX Mutant = 117 bp, MDX WT= 134 bp. Screening for the IL2R gamma mutation performed with the following primers (as from The Jackson Laboratory): (1) Wild-Type Reverse: CCTGGAGCTGGACAACAAAT, (2) Mutant-Reverse: GCCAGAGGCCACTTGTGTAG, (3) Common Forward: GTGGGTAGCCAGCTCTTCAG; with the following PCR protocols: NSG Wildtype: 94°C for 10 min, 30 x (94°C for 30 sec, 60°C for 1 min, 72°C for 1 min), 72°C for 2 min, 4°C hold. NSG Mutant: 94°C for 3 min, 30 x (94°C for 30 sec, 63°C for 45 sec, 72°C for 30 sec), 72°C for 5 min, 4°C hold. Product Sizes: NSG WT ~ 350bp, NSG Mutant ~ 175bp.

qRT-PCR Analysis. Cells were lysed with buffer RLT, and RNA was isolated using the RNeasy Plus Mini Kit (Qiagen) according to the manufacturer's protocol. cDNA was produced from total RNA using the SuperScript III First Strand Synthesis System (Life Technologies) per the manufacturer's protocol. Thermocycling and quantification were performed using the Mastercycler RealPlex 2 (Eppendorf). qRT-PCR assays were performed with iTaq Universal SYBR Green Supermix (Bio-Rad). Relative expression of individual genes compared to control groups was calculated by the delta delta cycle threshold ($\Delta\Delta$ -Ct) method with *GAPDH* or *RPS13* as the housekeeping gene. qRT-PCR primer sequences are available in Supplementary Table 5.

Supplemental Experimental References Cited

- Garcia, S.M., Tamaki, S., Xu, X., and Pomerantz, J.H. (2017). Human Satellite Cell Isolation and Xenotransplantation. *Methods in molecular biology* 1668, 105-123.
- Rozkalne, A., Adkin, C., Meng, J., Lapan, A., Morgan, J.E., and Gussoni, E. (2014). Mouse regenerating myofibers detected as false-positive donor myofibers with anti-human spectrin. *Hum Gene Ther* 25, 73-81.
- Shin, J.H., Hakim, C.H., Zhang, K., and Duan, D. (2011). Genotyping mdx, mdx3cv, and mdx4cv mice by primer competition polymerase chain reaction. *Muscle Nerve* 43, 283-286.
- Xu, X., Wilschut, K.J., Kouklis, G., Tian, H., Hesse, R., Garland, C., Sbitany, H., Hansen, S., Seth, R., Knott, P.D., *et al.* (2015). Human Satellite Cell Transplantation and Regeneration from Diverse Skeletal Muscles. *Stem cell reports* 5, 419-434.